 https://doi.org/10.3011/ESARDA.IJNSNP.2019.9

Optimisation and uncertainty estimation of the enrichment meter measurement technique for UF6 cylinders

Jean-Luc Dufour, Nicolas Pepin, Clement Deyglun and Anne-Laure Weber
IRSN
Fontenay-Aux-Roses, France
Email: jean-luc.dufour@irsn.fr, nicolas.pepin@irsn.fr, clement.deyglun@irsn.fr, anne-laure.weber@irsn.fr

Abstract:

IRSN carries out on-site non-destructive assay of nuclear material for domestic safeguards purposes in France. The paper presents the study of uncertainty components and the optimisation of the traditional uranium enrichment meter method, applied to UF6 in 30B and 48Y cylinders. This calibration-based gamma spectrometry technique measures the enrichment by quantifying the count rate in the 185.7 keV peak of uranium 235 in conditions of infinite thickness of the measured material. It is based on high resolution gamma spectrometry measurements coupled with an ultrasonic gauge. The calibration is performed with the spectrometer in a collimated geometry using U3O8 laboratory standards, whereas UF6 assays performed on-site are un-collimated in order to reduce the inspection time. Therefore, corrections need to be done to correct for the differences between laboratory and on-site measurements, and associated uncertainties have to be taken into account. A measurement of the container wall thickness is performed using an ultrasonic gauge in order to correct the gamma ray attenuation through the container wall. On-site tests and MCNP simulations were also performed to calculate a calibration transfer factor and evaluate the impact of different detector localisations on the count-rate acquisition. In addition, these tests showed the impact of the background, mainly due to the higher energy gamma rays of U-238 daughters that Compton scattered within UF6 and the detector. Finally, the measurement time was estimated, the use range of the technique was defined and the measured uranium enrichment uncertainty was calculated.

Keywords: enrichment; UF6; spectrometry; uncertainty; MCNP

1. Introduction

IRSN carries out on-site non-destructive assay of nuclear material as part of its mission of technical assistance to the Authority responsible for the protection and control of nuclear material in France. In order to enlarge its measurement control capabilities to uranium hexafluoride (UF_6) contained in 30B and 48Y cylinders, a study was conducted to develop a dedicated measurement system including software and mechanical support development. For this purpose, the traditional enrichment meter method was adapted to high resolution gamma spectrometry instrumentation and U_3O_8 standards available within IRSN nuclear material metrology laboratory.

High resolution portable gamma spectrometry measurements are routinely used to verify the U-235 enrichment in large UF_6 cylinders applying the calibration-based method known as the enrichment meter method in conjunction with an ultrasonic measurement of the container wall thickness [1-9]. Calibration between the uranium enrichment and the net count rate of the 185.7 keV gamma ray in a collimated geometry is performed at IRSN using U_3O_8 reference materials (U-235 from 0.7 % to 89 %). Due to the small dimensions of the reference materials (48 mm diameter by 26 to 33 mm filling height), the collimation is needed during calibration to fulfil the infinite thickness conditions at 185.7 keV. But the collimation cannot be applied on UF_6 cylinders on-site with reasonable container inspection time. It is therefore proposed here:

- to measure the net count rate of the 185.7 keV gamma ray from the UF_6 container in a non-collimated geometry in order to reduce the container inspection time on-site;
- to correct the differences in gamma-ray attenuation between the container wall of the U_3O_8 reference material and the container wall of the 30B and/or 48Y cylinder, in measurement geometry and in chemical composition between the reference materials and the item to be measured.

This paper presents the methodology and equipment implemented on-site within the framework of a qualification measurement campaign, and the study of uncertainty components. It also discusses some improvement prospects to reduce the measurement uncertainty.

2. Measurement principle

The enrichment meter method is based on the proportional relation between the U-235 enrichment value and the count rate for 185.7 keV gamma rays. If the detector views only a fraction of the uranium sample through a collimator, the 185.7 keV gamma rays from only a fraction of the total sample radiation reach the detector because of the strong absorption of uranium. This is the 'infinite-thickness' criterion (Table 1 lists the infinite-thickness values) [7]. The size

of this visible volume is independent of the U-235 enrichment and depends only on the collimated geometry and uranium's physicochemical properties.

Uranium compound	Density	Infinite thickness (cm)
Metal	18.7	0.26
UF6 (solid)	4.7	1.43
UO2 (powder)	2.0	2.75
U3O8 (powder)	7.3	0.74

Table 1: Mean free paths and infinite thickness for 185.7 keV gamma rays in uranium compounds [7].

This method presents the following limitations:

- only the near surface depth of the uranium sample is interrogated, which means that the material must be isotopically uniform;
- the available reference materials are small and need a narrow collimator to fulfil the infinite thickness requirements which require significant measurement time. Large measurement times are possible during the calibration in the laboratory, but not consistent with on-site measurements. Thus, a calibration transfer function (C_{TFE}) is calculated to measure the on-site sample without collimation, using calibration performed with collimation on reference materials;
- the calibration is performed with U_3O_8, but on-site UF_6 is measured. The coefficient *F/F'* corrects for the difference in chemical composition;
- if the measured material is embedded within a container, the gamma rays are attenuated by the container wall. The correction factor CF_C corrects for such attenuation;
- the detector efficiency can change between the calibration in the laboratory and the measurement on-site. The correction factor CF_ε corrects for the variations in efficiency.

Taking into account all these correction factors, U-235 enrichment *E* can be expressed as follows:

$$E = \left(A + B \times \left[R \times CF_c \times C_{TFE} \times CF_\varepsilon\right]\right) \times \left(\frac{F}{F'}\right) \quad (1)$$

where *A, B* are constants calculated during the calibration in collimated configuration with U_3O_8 reference materials. The term in brackets contains the measured net count rate at 185.7 keV obtained in non-collimated configuration (*R*) and correction factors. Each component is studied in the following paragraphs.

The measurement system implemented on-site contains a portable high resolution gamma spectrometer Detective type (AMETEK/ORTEC), a computer equipped with both Gammavision software (AMETEK/ORTEC) and in-house Enrichment software to drive the spectrum acquisition and apply the enrichment meter method, a shielding, a collimator, a spectrometer positioning system and an ultrasonic measurement system. The measurement set-up is shown in Figure 1.

3. Container wall impact

The component $CF_c = e^{-\mu_c T_c}$ corrects the attenuation of gamma rays by UF_6 container wall:

- μ_c the photon linear attenuation coefficient (bibliographical data);
- T_c the container wall thickness (measured using an ultrasonic thickness gauge).

The variance of the wall attenuation correction is given by the following expression:

$$u^2_{CF_c} = \left(\frac{\partial e^{-\mu_c T_c}}{\partial \mu_c}\right)^2 u^2_{\mu_c \rho_c} + \left(\frac{\partial e^{-\mu_c T_c}}{\partial T_c}\right)^2 u^2_{T_c} \quad (2)$$

$$\left(\frac{u_{CF_c}}{CF_c}\right)^2 = \left(\mu_c T_c\right)^2 \left[\left(\frac{u_{\mu_c}}{\mu_c}\right)^2 + \left(\frac{u_{T_c}}{T_c}\right)^2\right] \quad (3)$$

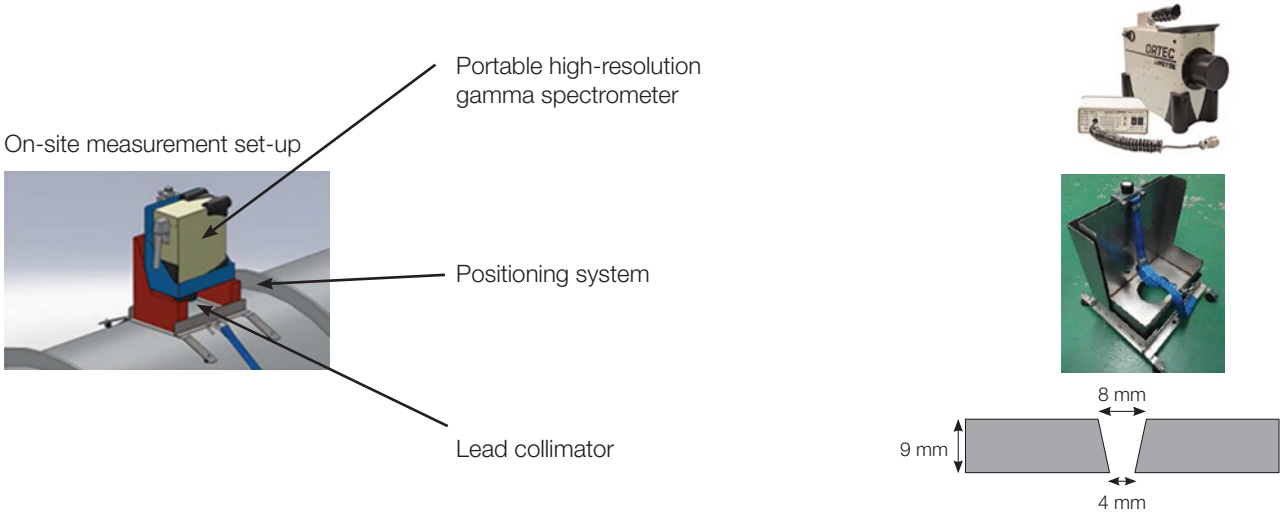

Figure 1: Measurement configuration.

Expressions and values of the parameters of Equation 2 and Equation 3 are presented in Sections 3.1 and 3.2. A numerical estimation of the variance is presented in Section 3.3.

3.1 Container wall measurement T_c

In the absence of a known reference standard stainless steel ASTM A516 Grade 65 type block, the ultrasonic gauge calibration was based on thickness measurements on the edge of UF_6 containers with a digital micrometer (0.001 mm resolution and ± 0.002 mm precision), considered as a reference. Thickness measurements with the ultrasonic gauge were then performed at the same location, adjusting the ultrasound speed according to the thickness value measured with the micrometer. Once the speed was fixed, the bias and precision of the ultrasonic gauge was evaluated (Figure 2).

The best measurements are obtained at a speed of 5925 m/s and the average wall thickness of measured 30B containers is 13.206 mm. The difference between the micrometer and the ultrasonic gauge measurements shows a uniform distribution. The precision (Equation 4) and the bias (Equation 5) are then calculated as follows [10]:

$$precision = \frac{\Delta_{max} - \Delta_{min}}{2\sqrt{3}} = 0.046 mm \quad (4)$$

$$bias = \frac{\sum_{i=1}^{n} \Delta_i}{n} = -0.043 mm \quad (5)$$

The overall uncertainty of the container wall thickness u_{Tc} (Equation 6) also includes components due to resolution, container paint thickness, ultrasound speed variations with temperature and container wall dilatation with temperature. These components are presented in Table 2.

$$u_{T_c} = \sqrt{u_{calib}^{\ 2} + u_{resol}^{\ 2} + u_{speed}^{\ 2} + u_{dilat}^{\ 2}} = 0.118 mm \quad (6)$$

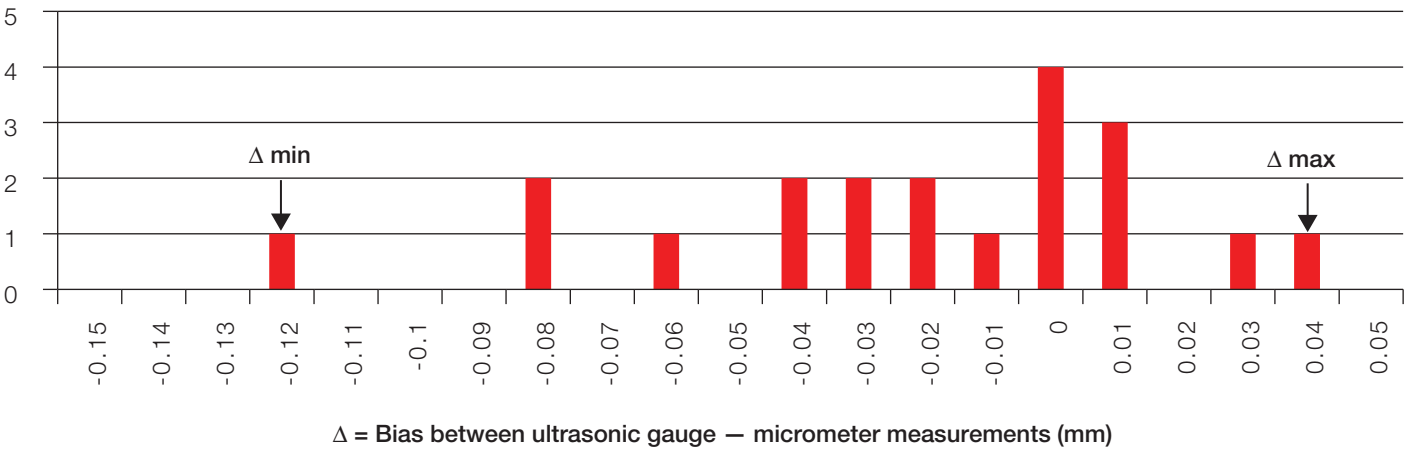

Figure 2: Distribution of the bias between the ultrasonic gauge and the micrometer during the measurement of the edge of containers.

Denomination	Comments	Evaluation
Calibration	Takes into account bias and precision from the calibration, but also additional bias sources such as the curvature of the container ($u_{curve} = 0.012mm$) and coating ($u_{coating} = 0.031mm$).	$u_{calib} = u_{precision} + \frac{\lvert u_{bias} + u_{curve} + u_{coating} \rvert}{\sqrt{3}}$ $u_{calib} = 0.096mm$
Resolution	The resolution of the ultrasonic gauge is 0.01 mm. At each measurement there could be an error of ± 0.01/2 mm.	Error is described by a uniform distribution: $u_{resol} = 0.01/2\sqrt{3}$ $u_{resol} = 2.887 \times 10^{-3} mm$
Variation of ultrasounds speed with temperature	The ultrasound's speed depends on the matter temperature. If the gauge is calibrated at 20 °C but the container wall is warmer, ultrasounds are slower and the wall appears thicker.	In winter, the container wall can be about –10 °C and in summer 60 °C (range of use defined by the manufacturer of the ultrasonic gauge) $u_{speed[-10°C;60°C]} = 0.068 mm$
Container wall dilatation with temperature	The dilatation of the wall decreases the matrix density and increases the thickness.	$u_{dilat} = 4.191 \times 10^{-3} mm$

Table 2: Components of the wall thickness measurement overall uncertainty.

3.2 Container wall attenuation correction

The typical chemical composition of 30B or 48Y containers (ASTM A516) and maximal fractions are presented in Table 3 [11].

C	Mn	Si	Al	P	S
0.18 (max = 0.26)	1.05 (0.85-1.20)	0.32	0.04	0.015 (max = 0.035)	0.008 (max = 0.035)

Table 3: Typical chemical composition of ASTM A516 Grade 65 and maximum [11].

μ_c for 185.7 keV gamma rays is calculated using XMuDat software [12] by assuming ASTM A516 Grade 65 and a density of 7.75. The coefficient is calculated for a typical composition and two 'extreme' compositions: μ_{min} is calculated with the minimal iron concentration and the maximum concentration for the other elements and μ_{max} is calculated with iron only.

$$\mu_{typical\ composition} = 1.222 cm^{-1}$$

$$\mu_{min} = 1.210 cm^{-1} \text{ and } \mu_{max} = 1.231 cm^{-1}$$

We assume a uniform distribution of μ between μ_{min} and μ_{max}, thus:

$$\mu_c = \frac{\mu_{max} + \mu_{min}}{2} = 1.221 cm^{-1} \quad (7)$$

and:

$$u_{\mu_c} = \frac{\mu_{max} - \mu_{min}}{2\sqrt{3}} = 0.006 cm^{-1} \quad (8)$$

3.3 Conclusion about the wall impact

The wall of the container absorbs gamma rays. The coefficient CF_c is applied in Equation 1 to correct these absorptions but it induces uncertainty. A numerical estimation of the variance (Equation 3) based on Equation 6 and Equation 8 is calculated using the data provided in the previous paragraphs. The variance of the wall attenuation correction u_{CF_c} depends on the measured wall thickness. An average thickness of 13.206 mm induces a variance $\frac{u_{CF_c}}{CF_c}$ of 1.644 %.

4. Impact of the detector location

The distribution of solid UF_6 inside the container is an important, but unknown, measurement parameter. MCNP6 simulations were performed to determine the influence of the detector position and the filling level on the enrichment measurement. On-site tests were also performed to check the simulation results.

4.1 MCNP6 simulations

MCNP6 [13] was used to model the gamma ray transport through UF_6 and 30B cylinder (Figure 3). Tally F5 (flux at a point) was used for the gamma ray spectrum detection, and only 185.7 keV gamma rays were generated. Many hypotheses are assumed for the model, as shown below:

H1. uniform properties of UF_6 (uniform chemical, isotopic composition and uniform density);

H2. gamma rays emitted by the gaseous UF_6 neglected;

H3. uniform wall thickness.

The impact of the detector location and the filling level on measurement results is studied by considering different detector locations on 30B container and filling level. Three locations (D1, D2 and D3) and different filling levels were studied as described in Figure 4.

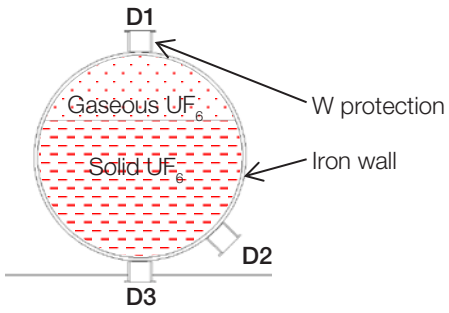

Figure 3: Cross section through a MCNP model of a 30B container.

As we can see in Figure 4, for filling levels higher than 30 cm (approximately 2180 kg) locations D1, D2 and D3 can be used interchangeably.

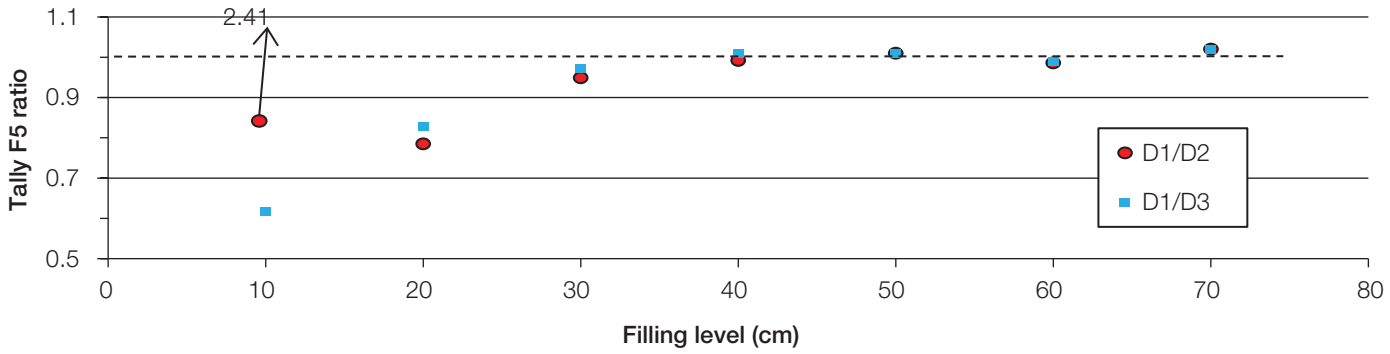

Figure 4: Ratios of tally F5 for different localisation (D1, D2 and D3) and filling levels.

4.2 On-site measurements

The influence of the detector position on the enrichment measurement is evaluated experimentally for seven detector locations along a 30B container (filled with 2200 kg of UF_6, at 1.41 % enrichment). At each detector position a thickness measurement is performed with the ultrasonic gauge to correct for the attenuation of the photons in the container wall. Locations and results are provided in Figure 5.

The relative standard deviation of the distribution of the count rate according to the detector position is around 1.1 %, which is less than the repeatability uncertainty (1.35 %).

4.3 Conclusion about the detector location

Simulation and on-site measurements show that detectors at the top and on the side of the container can be used interchangeably if the 30B container contains at least 2200 kg of UF_6. A measurement position at the top of the container and centred along the cylinder axis has the following two advantages:

- it is the most practical location to install the system;
- the acquisition is less impacted by the background generated by surrounding containers.

5. Correction due to the differences in chemical composition between reference materials and item to be measured

In the Equation 1 the coefficient $\frac{F}{F'}$ corrects the predicted enrichment from the differences in chemical composition between the reference material and the item to be measured (based on the data in Table 4). In case of UF_6 enrichment measurements based on a calibration performed with U_3O_8 samples, a correction factor of 1.02 needs to be applied to the enrichment value obtained from the calibration.

	Nuclear Material of Items Measured (Factor F)					
Nuclear Material of Calibration Standards (Factor F′)	**U**	**UC**	**UC_2**	**UO_2**	**U_3O_8**	**UF_6**
U (100 % U)	1.00	1.00	1.00	1.01	1.01	1.04
UC (95 % U)	1.00	1.00	1.00	1.01	1.01	1.03
UC_2 (91 % U)	0.99	1.00	1.00	1.00	1.01	1.03
UO_2 (88 % U)	0.99	0.99	1.00	1.00	1.00	1.03
U_3O_8 (85 % U)	0.99	0.99	0.99	1.00	1.00	1.02
UF_6 (68 % U)	0.96	0.97	0.97	0.98	0.98	1.00
U nitrate (47 % U)	0.92	0.92	0.93	0.93	0.93	0.95

Table 4: Material composition correction factors (F/F′) [7].

Table 4 does not provide any associated uncertainties $u_{F/F'}$. Taking two ratios F/F′ with small difference, for example $F/F'_1 = 1$ and $F/F'_2 = 1.01$, these two values are random values with means of 1 and 1.01 and associated uncertainties u_{F/F'_1} and u_{F/F'_2}. If we use the classic comparison test to compare the two means:

$$\frac{\left|F/F'_1 - F/F'_2\right|}{3\sqrt{u_{F/F'_1}^{\,2} + u_{F/F'_1}^{\,2}}} < 1 \qquad (9)$$

If the test of Equation 9 is true, the two means can be considered equal with a 'false alarm' probability of 0.26 %, and the difference is due to their associated uncertainties u_{F/F'_1} and u_{F/F'_2}. $\left|F/F'_1 - F/F'_2\right| = 0.01$ and the inequality becomes $3\sqrt{u_{F/F'_1}^{\,2} + u_{F/F'_1}^{\,2}} > 0.01$. If we assume the two uncertainties u_{F/F'_1} and u_{F/F'_2} are equal, i.e. $u_{F/F'_1} = u_{F/F'_2} = u_{F/F'}$ the inequality becomes $3\sqrt{2u_{F/F'}^{\,2}} > 0.01$ and $u_{F/F'} = \frac{0.01}{3\sqrt{2}} = 0.0024$.

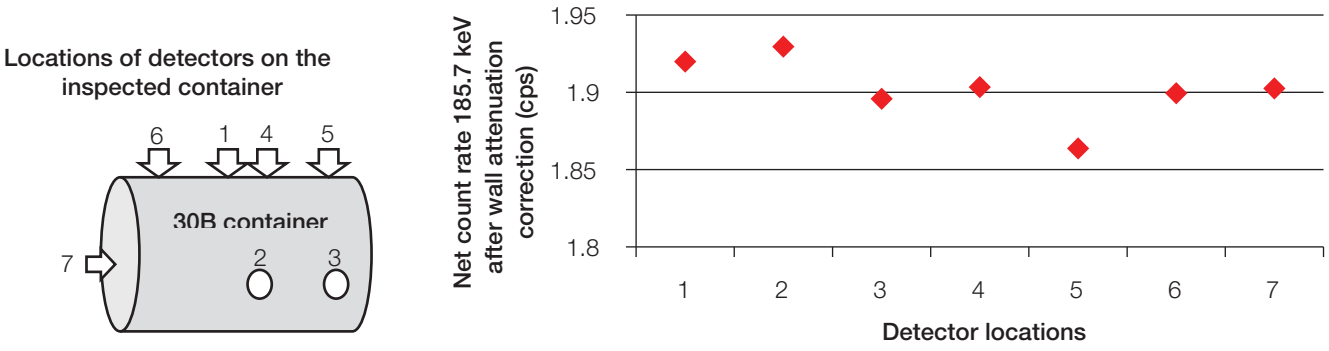

Figure 5: Impact of the detector localisation on the 185.7 keV gamma ray count rate (on-site measurements).

6. Correction due to the non-collimated geometry

Calibration with reference materials is performed in a collimated configuration to fulfil the infinite thickness requirements. By removing the collimator during on-site measurements on UF_6 cylinders, the calibration conditions are modified and then the counting rate measured for an unknown sample needs to be corrected with a calibration transfer function (C_{TFE}). C_{TFE} is derived from the ratio between the counting rates at 185.7 keV recorded in the two measurement configurations, with and without collimation. MCNP6 [13] simulations were performed to determine the C_{TFE} coefficient and were compared with on-site measurements.

6.1 MCNP6 simulations

MCNP6 was used to model the gamma-ray transport through UF_6, 30B cylinder and HPGe detector. A precise model of a 12 % relative efficiency p-type HPGe coaxial detector was created for photon detection (see Figure 6). Detector resolution and dead layers were determined by different experiments. The model was validated by comparing calculated and experimental full energy peak counting and FWHM for an Eu-152 source.

The gamma spectra are obtained using tally F8 (pulse height distribution). Collimated and non-collimated simulation results are presented in Figure 7.

C_{TFE} is derived from the ratio between the counting rates at 185.7 keV recorded in the two measurement configurations, with and without collimation, and is estimated at 0.00456. The associated uncertainty ($u_{C_{TFE}}$) includes components due to the trueness of the model, statistic and software deconvolution uncertainties $u_{C_{TFE}} = \sqrt{u_{model}^2 + u_{stat}^2 + u_{peak}^2} = 9.23\%$. These components are presented in Table 5.

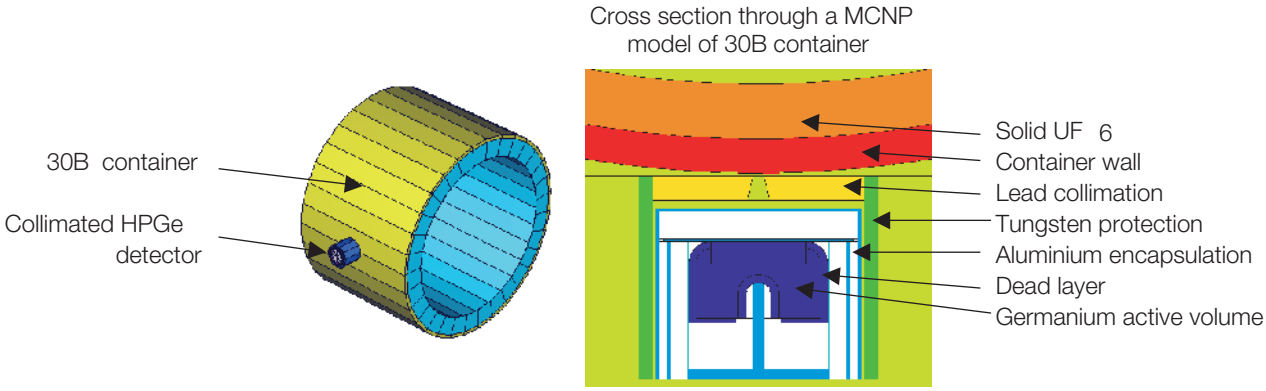

Figure 6: Model of the HPGe detector in collimated configuration (the lead collimator is replaced by air in the non-collimated configuration).

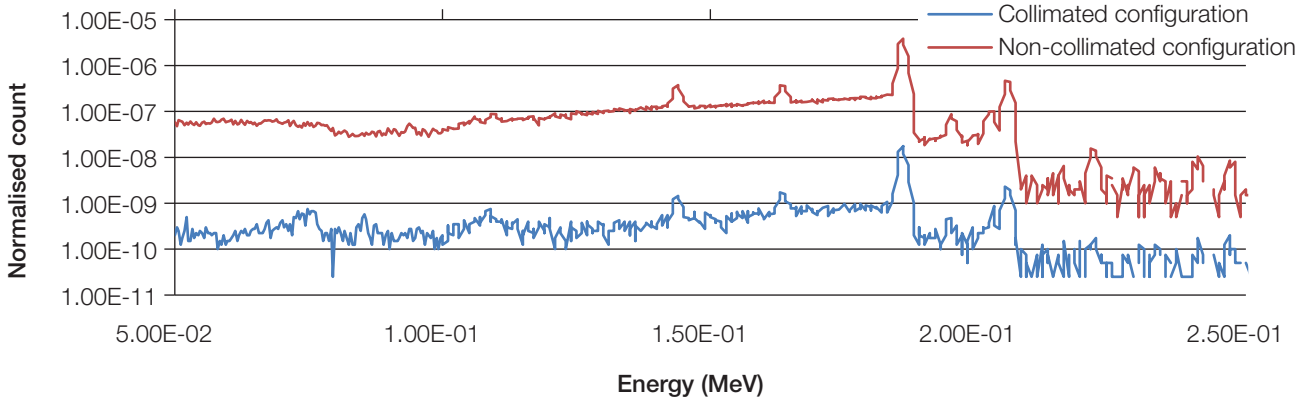

Figure 7: MCNP6 spectra of U-235.

Designation	Origin	Estimation	Comments
u_{model}	Adjustment of the MCNP model	4.65 %	Estimated with Eu-152 source between 80 keV and 1408 keV.
u_{stat}	Statistical uncertainty of Monte Carlo simulation	7.65 %	Mainly due to the low efficiency of the collimated configuration. Uncertainty could be reduced by increasing the calculation time
u_{peak}	Subtraction of the continuum background of the peak area	2.23 %	The simulation is free from the background continuum due to U-238

Table 5: Components of $u_{C_{TFE}}$.

6.2 Experimental C_{TFE}

Experimental measurements have been performed on one 30B container to estimate C_{TFE}. Three 120 seconds measurement time acquisitions are enough to get good counting statistics in the non-collimated configuration, but the collimated configuration needs a long measurement time (> 13 hours) to have good statistical uncertainty. The counting rates recorded in the collimated configuration on the side and at the top of the container are different due to the background from the other containers. C_{TFE} was calculated with the system at the top of the container, where the background contribution of the neighbour containers is small, and estimated at 0.00476.

C_{TFE} is derived from the ratio between the net counting rates at 185.7 keV recorded in the two measurement configurations, with and without collimation.

$$C_{TFE} = \frac{N_{with\ colli}}{t_{with\ colli}} / \frac{N_{without\ colli}}{t_{without\ colli}} \quad (10)$$

where $N_{with\ colli}$ is the number of detected 185.7 keV gamma rays for the collimated configuration and $t_{with\ colli}$ is the measurement time. Thus, the associated uncertainty $\left(\frac{u_{C_{FTE}}}{C_{FTE}}\right)^2$ is expressed as follows:

$$\left(\frac{u_{C_{TFE}}}{C_{TFE}}\right)^2 = \left(\frac{u_{N_{with\ colli}}}{N_{with\ colli}}\right)^2 + \left(\frac{u_{t_{with\ colli}}}{t_{with\ colli}}\right)^2 + \left(\frac{u_{N_{without\ colli}}}{N_{without\ colli}}\right)^2 + \left(\frac{u_{t_{without\ colli}}}{t_{without\ colli}}\right)^2 \quad (11)$$

The contribution of the measurement time uncertainties $\left(\frac{u_{t_{with\ colli}}}{t_{with\ colli}}\right)^2$ and $\left(\frac{u_{t_{without\ colli}}}{t_{without\ colli}}\right)^2$ is neglected, and in Equation 11 leads to:

$$\frac{u_{C_{TFE}}}{C_{TFE}} = 3.40\%$$

Despite a long measurement time, the relative uncertainty related to the counting rate with collimation is high (3.4 %) due to the poor signal-to-noise ratio. The noise is attributed to the Compton continuum of higher energy photons mainly coming from the large amounts of U-238 in the item and the *bremsstrahlung* emitted by its daughters.

6.3 Conclusion about C_{TFE}

MCNP6 was used to estimate the calibration transfer function correction, but modelling uncertainties and simulation time induce significant uncertainties. In the end, the experimental C_{TFE} has a better uncertainty. C_{TFE} is needed because on-site measurements and calibration conditions are different.

7. Calibration and inverse calibration

The reference materials available within the laboratory are four U_3O_8 powder samples, infinitely thick with respect to the 185.7 keV gamma emission, embedded in a POMC (Acetal Copolymer) container. Their characteristics are summarised in Table 6.

U_3O_8 mass (g)	Enrichment (wt %)	Enrichment Unc. (wt %)
120.9	0.714	0.005
114.73	3.038	0.018
106.81	29.187	0.018
104.74	89.303	0.018

Table 6: Reference materials ^{235}U enrichment.

The calibration is performed in a collimated geometry as follows: the reference material is placed on the collimator, which is itself positioned against the front face of the germanium detector, both of them being centred on the axis of the coaxial germanium detector. The calibration consists in measuring the net counting rate at 185.7 keV (R_i) for each reference material using the ROI (Region Of Interest) report option of the Gammavision software. The correction factor CF_r is then applied to correct it from the attenuation of the wall thickness, and a weighted least-squares linear regression is applied to the couples (R_i, E_i),E_i being the U-235 enrichment value given by the certificate. The measurement time is defined in order to get a counting statistics of around 1 % in the 185.7 keV net peak area.

The correction factor due to the attenuation from the reference material container wall (CF_r) is estimated experimentally by performing the ratio $CF_r = \frac{R_0}{R}$, where R_0 is the counting rate measured at 184.4 keV with a ^{166m}Ho source and R is the counting rate measured when an equivalent container wall is installed between the detector and this source.

The weighted linear least-squares regression is applied to the couples (R_i, E_i), using as weight the inverse of the variance of the counting rate ($g_i = \frac{1}{s_i^2}$) [14,15]. The coefficients a, b and R are given by the following expressions:

$$b = CF_r \frac{\sum g_i \sum g_i E_i R_i - \sum g_i E_i \sum g_i R_i}{\sum g_i \sum g_i E_i^2 - \left(\sum g_i E_i\right)^2} \quad (12)$$

$$R = \frac{\sum g_i R_i CF_r}{\sum g_i} = CF_r \frac{\sum g_i R_i}{\sum g_i} \quad (13)$$

and:

$$a = R - bE \quad (14)$$

Equation 12 and Equation 14 lead to calibration factors a = – 0.011496151 and b = 0.806211927.

The enrichment of an 'unknown' item can then be predicted using the inverse calibration.

$$R = a + b \times E \quad (15)$$

$$E = A + R \times B \quad (16)$$

where R is the measured net counting rate at 185.7 keV obtained in non-collimated configuration, E is the unknown U-235 enrichment, $A = -\frac{a}{b}$ and $B = \frac{1}{b}$.

8. Overall uncertainty

The enrichment measurement uncertainty is calculated as follows:

$$u_E = \sqrt{u^2_{Calibration} + u^2_{\frac{F}{F'}} + u^2_{Trueness}} \quad (17)$$

where:

- $u^2_{Calibration}$ depends mainly on the regression model, counting rates uncertainties and corrections applied to these counting rates. Enrichment can be expressed as follows, $E_{after\ \frac{F}{F'}\ correction} = E_{before\ \frac{F}{F'}\ correction} \times \frac{F}{F'}$, and thus $u^2_{Calibration} = E^2_{after\ \frac{F}{F'}\ correction} \left(\frac{u_{E_{before\ \frac{F}{F'}\ correction}}}{E_{before\ \frac{F}{F'}\ correction}} \right)^2$
- $u^2_{\frac{F}{F'}}$ is evaluated based on a difference of 0.01 between the ratios of two matrix material composition correction factors (Section 5);
- $u^2_{Trueness}$ is evaluated from the known enrichment-item measurements. It is calculated considering a rectangular distribution of the bias of n assays, i.e. $u_{Trueness} = \frac{\left| \sum_{i=1}^{n} \left(E_{Reference_i} - E_{Measured_i} \right) \right|}{n\sqrt{3}}$

The inverse calibration is applied to the corrected count rate $R_{corrected}$ in order to determine the predicted enrichment $\left(E_{before\ \frac{F}{F'}\ correction} \right)$:

$$R_{corrected} = R\, C_{TFE}\, CF_c\, C_\varepsilon \quad (18)$$

$$u_{R_{corrected}} = R_{corrected} \sqrt{\left(\frac{u_R}{R}\right)^2 + \left(\frac{u_{CF_c}}{CF_c}\right)^2 + \left(\frac{u_{C_{TFE}}}{C_{TFE}}\right)^2 + \left(\frac{u_{C_\varepsilon}}{C_\varepsilon}\right)^2} \quad (19)$$

Based on Equation 16 and Equation 18, the predicted the enrichment is expressed as follows:

$$E_{before\ \frac{F}{F'}\ correction} = \left(\frac{R \times CF_C \times C_{TFE} \times C_\varepsilon - a}{b} \right) \quad (20)$$

The estimation of the predicted enrichment uncertainty before $\frac{F}{F'}$ correction $u_{E_{before\ \frac{F}{F'}\ correction}}$ is calculated from the confidence interval of the predicted enrichment $IC_{Regression}$ [14,15]. Assuming that the confidence interval variable follows a rectangular probability law, the uncertainty associated with the predicted enrichment is given by $u_{E_{before\ \frac{F}{F'}\ correction}} = \frac{IC_{Regression}}{2\sqrt{3}}$.

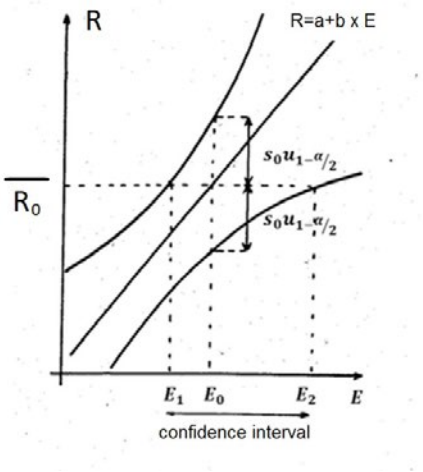

Figure 8: The enrichment confidence interval.

The enrichment confidence interval $IC_{Regression}$ is limited by E_1 and E_2 (see Figure 8). These boundaries are calculated through the intersection between $R = R_0$ and $R = a + bE \pm S_0 u_{1-\frac{\alpha}{2}}$, where $u_{1-\frac{\alpha}{2}}$ is a normal restricted variable ($u_{1-\frac{\alpha}{2}} = 3$ induces a false alarm risk of 0.26 %).

E_1 and E_2 are calculated by resolving the two following equations:

$$R_0 = a + bE_0 + S_0 u_{1-\frac{\alpha}{2}} \quad (21)$$

$$R_0 = a + bE_0 - S_0 u_{1-\frac{\alpha}{2}} \quad (22)$$

with $S_0 = \sqrt{S^2_{R_{corrected}} + \frac{1}{\sum g_i} + \frac{\left(E_0 - \bar{E}\right)^2 \sum g_i}{\sum g_i \sum g_i E_i^2 - \left(\sum g_i E_i\right)^2}}$

The confidence interval $IC_{Regression}$ is then made symmetrical by calculating the boundaries $E_1 = E_0 - Max\left(\left|E_0 - E_1\right|, \left|E_0 - E_2\right|\right)$ and $E_2 = E_0 + Max\left(\left|E_0 - E_1\right|, \left|E_0 - E_2\right|\right)$.

9. Conclusions

The on-site measurement of UF_6 containers and numerical simulations contributed to the validation of the U-235 enrichment calibration-based method relying on the small dimension reference materials available at IRSN. Only small U_3O_8 reference materials are available at IRSN so that collimation is needed to fulfil the infinite thickness conditions during calibration. On the other hand, in order to make

on-site verifications compatible with time inspection constraints, the 185.7 keV net counting rate is measured in a non-collimated geometry. Therefore, a transfer function between the two different geometries is applied. This correction was estimated both experimentally and numerically, with good agreement between the two of them.

The measurement uncertainty, around 5 % for low enriched uranium and 10 % for depleted uranium, could be improved in the future. Peak-fitting algorithms could be investigated in order to extract net peak area from a high background continuum with better accuracy. The geometry transfer function coefficient could be useless if the calibration was performed with a large uranium reference sample.

10. References

[1] IAEA, *Safeguards Techniques and Equipment*, 2011 edition, *International Nuclear Verification Series No 1 (Rev. 2)*.

[2] *Standard test method for measurement of 235U fraction using enrichment meter principle*, norm ASTM C1514, 2002.

[3] *International target values 2010 for measurement uncertainties in safeguarding nuclear materials*, STR-368, IAEA, Vienna, 2010.

[4] Kull, L. A., Ginaven, R. O. and Glancy, J. E., 'A simple gamma spectrometric technique for measuring isotopic abundances in nuclear materials', *Atomic Energy Review*, 1976.

[5] Kull, L. A. and Ginaven, R. O., *Guidelines for gamma-ray spectroscopy measurements of ^{235}U enrichment*, Technical Support Organization, Brookhaven National Laboratory, Upton, New York, 1974.

[6] Carchon, R., *IAEA Verification Techniques on UF6 Shipping Cylinders*, 2007.

[7] Reilly, D., Ensslin, N., Smith, H. and Kreiner, S., *Passive Nondestructive Assay of Nuclear Materials*, NUREG/CR-5550, LA-UR-90-732, 1991.

[8] Mortreau, P. and Berndt, R., *Handbook of gamma spectrometry methods for non-destructive assay of nuclear materials*, European Commission Joint Research Centre, 2006.

[9] Montgomery, J. B., 'Enhanced techniques and improved results in 235U enrichment measurement of large UF6 cylinders by portable germanium spectrometer', *Journal of Nuclear Materials Management*, Vol. 34, No 2, 2006.

[10] Feinberg, M., *Labo-Stat: Guide technique d'accréditation pour l'évaluation des incertitudes de mesure en biologie médicale*, SH GTA 14 Rev00.

[11] *Specification for pressure vessel plates, carbon steel, high strength, for moderate and lower temperature service*, SA-516/SA-516M Section II, Part A, 2009.

[12] Nowotny, R., *XMuDat: Photon Attenuation Data on PC*, version 1.0.1, Institut für Biomedizinische Technik und Physik, University of Vienna, AKH-4L, 1998.

[13] Pelowitz, D. B. (ed.), *MCNP6 User's Manual — Version 1.0*, Los Alamos National Laboratory report LA-CP-13-00634 (May 2013).

[14] CETAMA, *Statistique appliquée à l'exploitation des mesures*, Ed. MASSON, second edition, 1986.

[15] Neuilly, M., *Modélisation et estimation des erreurs de mesures*, CETAMA, 1993.